NUMERICAL ANALYSIS OF THE EFFECTS OF CHANGEABLE TRANSVERSE AND LONGITUDINAL PITCHES AND POROUS MEDIA INSERTS ON HEAT TRANSFER FROM AN ELLIPTIC TUBE BUNDLE

Haniyeh Razzaghi

Young Researchers and Elite Club, Karaj Branch, Islamic Azad University, Karaj, Iran

Mohammad Layeghi

Faculty of Natural Resources, University of Tehran, Karaj, Iran; e-mail: mlayeghi@ut.ac.ir

Siavash Goodarzi

Takestan Branch, Islamic Azad University, Takestan, Iran

Hossein Lotfizadeh

Faculty of Mechanical Engineering, Karaj Branch, Islamic Azad University, Karaj, Iran

In this paper, effects of changeable transverse and longitudinal pitches and porous media inserts on overall heat transfer from an elliptic tube bundle are studied numerically. Governing equations used for the analysis of fluid flow inside the porous media inserts are Darcy-Brinkman-Forchheimer equations, and for the fluid flow without porous inserts are classical Navier-Stokes equations. A finite volume code is used to solve the governing equations. The tube bundle consists of 10 rows of elliptical tubes 3.17 cm in major diameter and 1.4 cm in minor diameter in a staggered arrangement. Aluminum foams are used as porous media inserts between the tubes with three different porosities. It is shown that the use of the aluminum foam enhances heat transfer significantly (more than 50% in some cases). However, the pressure drop increases as the Reynolds number grows. The differences among various cases are also discussed. Finally, it is shown that the overall heat transfer efficiency increases more effectively by increasing the transverse pitch with respect to the longitudinal and diagonal pitches while the flow regime remains laminar.

Keywords: elliptic tube bundle, heat transfer, pitches, aluminum foam, efficiency

1. Introduction

Elliptic tube bundles and their heat transfer augmentation techniques have been recently noted due to their low pressure drop and applications in heat exchanger industry. The aim of enhanced heat transfer is to encourage or accommodate higher heat fluxes. There are several methods to improve the efficiency and performance of heat exchangers. Some common methods which are purely convection-based are: increasing heat flow per unit surface area, increasing the number of tubes or improving tube arrangements and shapes. However, each of these methods could prove difficult when considering manufacturing noise or tolerances, cost or weight. Novel methods include enhancing heat transfer from a given surface via inserting porous media when dealing with forced convection in a laminar flow such as dealing with plate fins in a tube. Furthermore, the effect of changes in the tube geometry and arrangements on the overall heat transfer and pressure drop of the plate fin and tube heat exchanger appears to yield desirable heat transfer augmentation.

A significant body of work has been published on various tube geometries and their arrangements augmenting tube heat transfer. Heat exchangers with finned elliptical tubes were studied experimentally by Jang and Yang (1998). They showed that the observed heat transfer augmentation when compared to that induced by circular tubes also resulted with a relative pressure

drop reduction of up to 30%. Webb (1980) believed that the performance advantage of elliptical tubes results from their lower pressure drop due to smaller wake regions behind the tubes. Marchi (2007) numerically studied the effect of distance between the tubes, aiming to optimize geometrical configuration of the heat exchanger at two Reynolds numbers 50 and 100. Rocha *et al.* (1997) developed a hybrid mathematical model for finned circular and elliptic tubes arrangements based on energy conservation and on heat transfer coefficients obtained experimentally by a naphthalene sublimation technique through a heat and mass transfer analogy. They obtained numerically the fin temperature distribution and fin efficiency in one and two row elliptic tubes and plate fin heat exchangers. The fin efficiency results were then compared to the results of Rosman *et al.* (1984) for the plate fin and circular heat exchangers, and a relative fin efficiency gain of up to 18% was observed with the elliptical arrangement. The same sublimation technique was used for plate fin heat exchangers with circular tubes by Kim and Song (2002). Torikoshi *et al.* (1994) investigated a plain fin and a tube heat exchanger numerically. Bordalo and Saboya (1999) reported pressure drop measurements comparing elliptic and circular tubes and plate fin heat exchangers configurations with one, two, and three-row arrangements. Reductions of up to 30% of the loss coefficient were observed in favor of the elliptic configuration. The comparison was performed between circular and elliptic arrangements with the same flow obstruction cross-sectional area for Reynolds numbers between 200 and 2000 which covered the air velocity range of interest for air conditioning applications. It was further observed that the reduction in pressure drop was higher as the Reynolds number increased and was negligible when the Reynolds number reached to 200 for the three-row arrangement. Matos *et al.* (2004a,b) carried out a three-dimensional numerical and an experimental investigation of geometric optimization to maximize the forced convection heat transfer rate between a bundle of finned tubes. The air flow regime was laminar and the Reynolds number was 852 and 1065 in their studies. Furthermore, the effects of tube-to-tube spacing, eccentricity, and fin-to-fin spacing were investigated. A heat transfer gain of up to 20% was reported for the optimal elliptic arrangement in comparison with the optimal circular one.

Li *et al.* (2006) studied two-dimensional fluid flow and heat transfer between constant temperature elliptical tubes with axis ratios of 0.3, 0.5 and 0.8. The flow regime was laminar and the Reynolds number ranged from 500 to 10,000. Their results showed that the elliptical cylinder with an axis ratio of 0.5 and zero angle of attack reduces the pressure drop by 30-40% compared to a circular cylinder. Also, the Nusselt number was found to be 15% lower than the circular tube. Tao *et al.* (2007) investigated laminar fluid flow and heat transfer characteristics for circular and elliptic tube arrangements numerically. They obtained a 30% gain of the heat transfer and, consequently, 10% increase in the friction factor. Recently, Ibrahim and Gomaa (2009) have investigated thermo-fluid characteristics of an elliptic tube bundle in cross flow. They investigated the turbulent flow through a bundle of elliptic tubes heat exchanger experimentally and numerically with a particular reference to the circular tube bundle. Their results showed that increasing the angle of attack clockwise until 90° enhances the convective heat transfer coefficient considerably. The best thermal performance of elliptic tube heat exchangers was qualified with the lower values of axis ratio, angle of attack, and Reynolds number.

There is, however, only a limited number of published works relating to the heat transfer enhancement from a tube bundle using porous materials. Pavel and Mohammad (2004) reported experimental investigation of the effect of heat porous matrix inserted in a pipe on the rate of pipe heat transfer while considering also the flow case where no porous material was inserted in the pipe. Bhattacharya and Mahajan (2002) presented experimental results on forced convective heat transfer in finned metal foam heat sinks. Experiments were conducted on aluminum foams of 90% porosity and two different pore sizes (5 PPI and 20 PPI) with one, two, four, and six fins. Their results showed that heat transfer is significantly enhanced when fins are incorporated in metallic foams. Their study also showed that increasing the number of fins and PPI leads

to heat transfer enhancement. However, due to higher PPI, the pressure drop is much higher at a particular air velocity. Tadrist *et al.* (2004) investigated the use of aluminum foam for compact heat exchangers. The porosities were in the range of $\varepsilon > 0.9$. They experimentally determined the flow parameters (and used an Ergun type correlation between the pressure drop and the fluid velocity. Mahdi *et al.* (2006) experimentally studied the performance of CPU heat exchangers and compared it with aluminum-foam heat exchangers in natural convection using an industrial setup. Their results showed that by employing aluminum-foam CPU heat exchangers, the thermal resistance decreases more than 70%. Also, the aluminum-foam heat exchangers reduced the overall weight. Shih *et al.* (2006) studied the effect of height on cooling performance of aluminum foam heat sinks under impinging–jet flow condition. They reported that when the height-to-diameter ratio of aluminum foam heat sinks reduces from 0.92 to 0.15, the Nusselt number of aluminum foam first increases and then decreases, and by decreasing the porosity and pore density, the Nusselt number increases and convective heat transfer is enhanced. Studies by Bastawros (1998) showed the efficacy of metallic foams in forced convective heat removal in electronic cooling applications. Layeghi (2008) numerically studied forced convective heat transfer from a staggered tube bundle with various low conductivity wooden porous media inserts at the maximum Reynolds number 100 and 300. He showed that inserting wooden porous media can increase heat transfer, and high conductivity porous media are very effective for heat transfer enhancement. Recently, Thirumalai Kannan and Senthil Kumar (2011) numerically studied heat transfer and flow in plate-fin and tube heat exchangers with different shaped vortex generators mounted behind the tubes. The effects of different span angles ($\alpha = 30°$, $45°$ and $60°$) were investigated in detail for the Reynolds number ranging from 500 to 2500. The results indicated that the triangle shaped winglet is able to generate longitudinal vortices and improves the heat transfer performance in the wake regions. The case of $\alpha = 45°$ provided the best heat transfer augmentation than the rectangle shape winglet generator in the case of inline tubes. Simo Tala *et al.* (2012) studied the effect of iso-sectional tube shape modification (from circular to elliptic) on the air-side thermal hydraulic characteristics and entropy production rate in three geometrical configurations of the plate fin and tube heat exchanger and two airflow velocities. The results showed that the reduction of the tube ellipticity significantly increases the thermal hydraulic performance of the heat exchanger up to 80% in comparison with the circular tube. Chen and Lai (2012) investigated the experimental and numerical inverse methods to determine the average heat transfer coefficient and heat transfer coefficient under the isothermal situation on a vertical square fin of the two-row plate finned-tube heat exchangers with four circular tubes for the staggered arrangement and various air velocities and fin spacings. The results showed that both heat transfer coefficients increases with the air velocity and fin spacing for the staggered arrangement. T'Joen *et al.* (2010) studied a new heat exchanger design with metal foams. It included a single row of aluminum tubes covered with thin layers (4-8 mm) of metal foam. The results indicated a strong need for a cost-effective and efficient brazing process to connect metal foams to the tube surfaces. Talaat and Abdalla (2009) studied thermofluid characteristics of the elliptic tube bundle in cross flow experimentally and numerically. The investigation covered the effects of key design parameters of Reynolds numbers (5600-40,000), minor-to-major axis ratios (0.25, 0.33. 0.5 and 1) and flow angles of attack (0-150). The results showed that increasing the angle of attack clockwise until 90° enhances the convective heat transfer coefficient noticeably. The maximum and the minimum thermal performance under constraint of a fixed pumping power or a mass flow rate were obtained at a zero and 90° angle of attack, respectively. Horvat *et al.* (2006) and Horvat and Mavko (2006) performed transient numerical simulations of the fluid and heat fluid for a number of heat exchanger segments with cylindrical, ellipsoidal, and wing-shaped tubes in a staggered arrangement. For each of almost 100 analyzed cases, time distributions of the Reynolds number, drag coefficient, and Stanton number were recorded. The comparison of the collected data allowed drawing more general conclusions on the efficiency and

stability of the heat transfer process in tube bundles. Berbish (2011) recently studied turbulent heat transfer and flow behavior around four staggered elliptic cylinders in cross flow numerically and experimentally. The elliptic cylinders examined had an axis ratio of 1:2, and they were arranged with the zero angle of attack to the upstream flow. The effects of the Reynolds number, longitudinal, and transversal spacing ratios were examined.

This work focuses on heat transfer augmentation by porous media inserts between the tubes of a staggered tube bundle and by changes of distances between the tubes at Reynolds numbers in the range 50-300. The tube bundle is an industrial one with changeable transverse and longitudinal pitches in the range ±12%. The differences among various cases are also discussed.

2. Problem definition, geometry, and governing equations

2.1. Investigating the effect of porous aluminum foam on the tube heat transfer

Aluminum foams are inserted between tubes in a tube bundle shown in Fig. 1 and their effects on the tube bundle heat transfer is examined. Results are also compared with the available data on the tube bundle heat transfer in the absence of such porous inserts. The differences between the two cases are discussed.
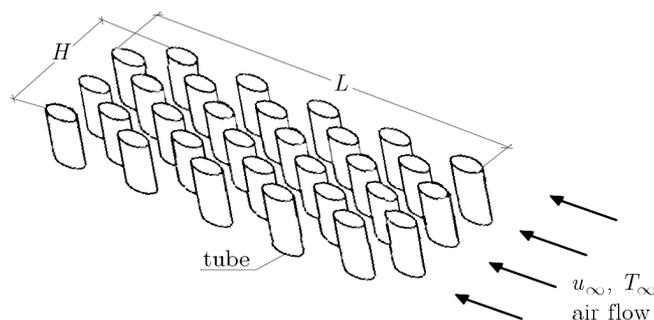
Fig. 1. Schematic of a tube bundle with elliptical tubes

2.2. The effect of the distance between the tubes

Since the industrial tube bundle considered has changeable tube pitches, the effect of tube spacing on the tube bundle heat transfer is also investigated in order to obtain the maximum heat transfer efficiency.

Two sets of governing equations are used for the study of air flow and heat transfer around elliptic tube bundles with and without metal foam inserts. Based on Zukauskas (1972) observation at Re < 1000, fluid flow around a tube bank can be considered to be dominantly laminar despite large scale vortices in the recirculation region behind the tubes. Since the Reynolds number range is below 300, the air flow is assumed to be laminar. A two-dimensional unit cell symmetrical model shown in Fig. 2 is used as the solution domain. It should be noted that due to high computational complexity, a two-dimensional model is considered. The tube bundles used in the numerical analyses have 10 row elliptic tubes.

Figure 3 shows the solution domain used for the study of air flow and heat transfer between the tubes without metal foam inserts.

The steady state laminar and incompressible air flow and the heat transfer around tubes without metal foam inserts are described by the classical Navier Stokes equations together with the energy equation. These equations are as follows:
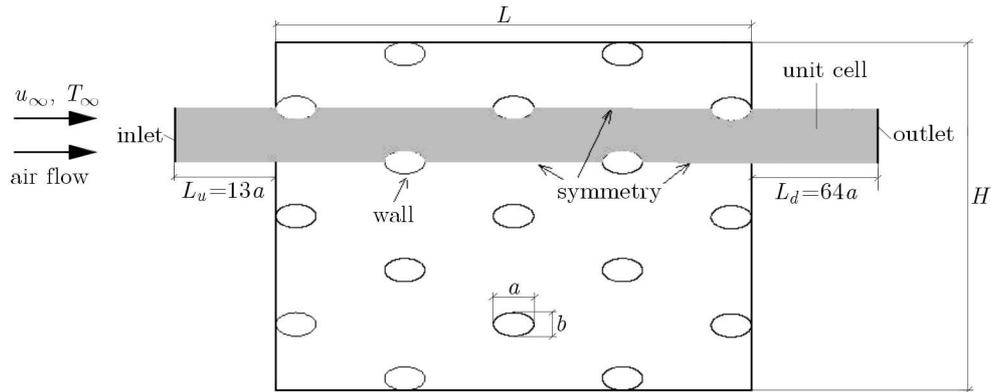
Fig. 2. Schematic geometry of the staggered arrangement of tubes and the solution domain (in gray color)
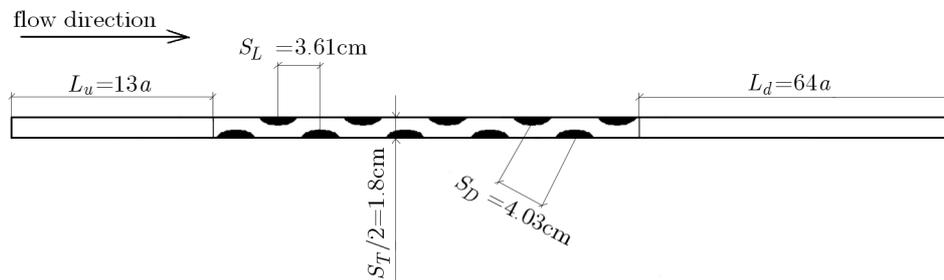
Fig. 3. The solution domain and the tube bundle boundary definition without metal foam inserts

— continuity equation

$$\nabla \cdot \mathbf{V} = 0 \tag{2.1}$$

— momentum equation

$$\rho \mathbf{V} \cdot \nabla \mathbf{V} = -\nabla P + \mu \nabla^2 \mathbf{V} \tag{2.2}$$

— energy equation

$$\rho C_p \mathbf{V} \cdot \nabla T = k \nabla^2 T + \mu \Phi \tag{2.3}$$

where in Eqs. (2.1)-(2.3) $\mathbf{V} = [u, v]$ is the flow velocity vector, P and T are flow pressure and temperature, respectively, C_P, ρ, μ and k are specific heat at constant pressure, density, viscosity of the fluid, and thermal conductivity, respectively, Φ is the dissipation function and it represents the time rate at which energy is being dissipated per unit volume through the action of viscosity. For an incompressible flow, it is written as follows

$$\Phi = 2\Big[\Big(\frac{\partial u}{\partial x}\Big)^2 + \Big(\frac{\partial v}{\partial y}\Big)^2\Big] + \Big(\frac{\partial u}{\partial y} + \frac{\partial v}{\partial x}\Big)^2 \tag{2.4}$$

Figure 4 shows the solution domains used for the study of air flow and heat transfer between the tubes with metal foam inserts.

The steady state laminar and incompressible air flow in metal foam inserts between tubes by assumption of the isotropic saturated porous medium with constant properties and in local thermal equilibrium conditions can be written as follows:

— continuity equation

$$\nabla \cdot \mathbf{V} = 0 \tag{2.5}$$
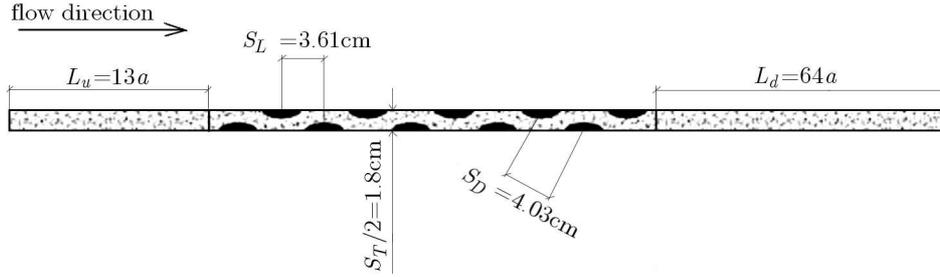
Fig. 4. The solution domain and the tube bundle boundary definition with porous inserts

— momentum equation

$$\frac{\rho_f}{\varepsilon}\nabla\Big(\frac{\mathbf{V}\cdot\mathbf{V}}{\varepsilon}\Big) = -\nabla P + \frac{\mu}{\varepsilon}\nabla^2\mathbf{V} - \frac{\mu}{k}\mathbf{V} - \frac{C_F\rho_f}{\sqrt{K}}|\mathbf{V}|\mathbf{V} \tag{2.6}$$

— energy equation

$$\rho_f C_P \mathbf{V}\cdot\nabla T = \Big[(k_{eff} + k_{D,x})\frac{\partial^2 T}{\partial x^2} + (k_{eff} + k_{D,y})\frac{\partial^2 T}{\partial y^2}\Big] \tag{2.7}$$

where in Eqs. (2.5)-(2.7) $\mathbf{V} = [u, v]$ is the Darcy velocity vector and u, v are the Darcy velocity components, C_F is dimensionless form-drag constant, T is temperature, and P is static pressure. Here, we assume $C_F = 0.1$ which is an average value for many types of foams. ε and K are porosity and permeability of the porous medium, respectively, k_{eff} is the effective thermal conductivity of porous medium. It is the volume average of the fluid medium (air) and solid medium (aluminum) conductivities, $k_{eff} = \varepsilon k_f + (1 - \varepsilon)k_s$. The indices f and s refer to the fluid and solid part of the porous medium, respectively. $k_{D,x}$, $k_{D,y}$ are the longitudinal and transverse thermal dispersion conductivities in the x, y directions, respectively. At high pore Reynolds numbers in nearly parallel flows, they can be correlated as a linear function of the Peclet number. Since the porous medium is assumed to be isotropic, $k_{D,x} = k_{D,y}$, the thermal dispersion can be then obtained by the following equation

$$\frac{k_D}{k_f} = C_F\mathrm{Pe}_m = \frac{C_T U_m d_p}{\alpha_f} \tag{2.8}$$

where in the above equation, Pe_m is the Peclet number based on the pore diameter d_P and the mean velocity U_m. The coefficient C_T depends on the porous medium structure and distance from solid walls. $\alpha_f = k_f/(\rho C_P)_f$ is the thermal diffusivity of the fluid.

3. Computational domain and boundary conditions

The computational domain has width of $S_T/2$ and length of L_u+L+L_d as shown in Figs. 3 and 4. The elliptical tubes have the major diameter ($a = 3.17\,\mathrm{cm}$) and minor diameter ($b = 1.4\,\mathrm{cm}$). The staggered arrangement is in form of an equilateral triangle with $S_D/b = 2.87$, $S_L/a = 1.138$, $S_T/b = 2.57$ where S_T, S_L, S_D are the transverse, longitudinal and diagonal distances among the centers of adjacent tubes, respectively.

A combination of the inlet, outlet, wall and symmetry boundary conditions is applied to the computational domain in order to reasonably represent physical characteristics of the flow with heat transfer through the tube arrays (Fig. 2 and Table 1). For the elliptical tube surfaces, the no-slip boundary conditions were assigned. The constant temperature boundary condition is applied to the heated wall ($T_w = 400\,\mathrm{K}$), whereas the symmetry lines are insulated. At the

inlet, constant temperature $(T_\infty = 300\,\mathrm{K})$ and a uniform profile are prescribed for the velocity. At the outlet, only the value of static pressure is specified; the remaining flow variables are extrapolated from within the flow domain itself. A single domain approach is used to solve the convective heat transfer problem. Table 1 gives the boundary conditions used in the solution.

Table 1. Boundary conditions for the computational domain

Boundary condition	U	V	T
Inlet	$U = U_\infty$	$V = 0$	$T = T_\infty$
Outlet	$\frac{\partial U}{\partial x} = 0$	$V = 0$	$\frac{\partial T}{\partial x} = 0$
Symmetry	$\frac{\partial U}{\partial y} = 0$	$V = 0$	$\frac{\partial T}{\partial y} = 0$
Tube surface	$U = 0$	$V = 0$	$T = T_W$

4. Method of solution and grids

Equations (2.1)-(2.3) and (2.5)-(2.7) have been solved separately using a finite volume code based on a collocated grid system. The grid consistes of triangular cells around tubes and quadratic cells in the upstream and downstream regions and near tube walls. The computational mesh around the typical elliptic tubes is shown in Fig. 5.
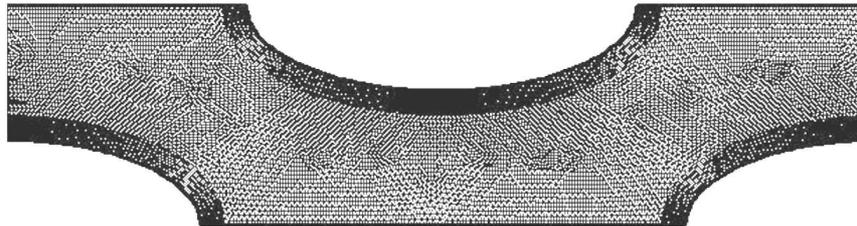
Fig. 5. Computational mesh around the elliptic tubes

Three different mesh sizes with 50000, 200000, and 1800000 computational cells were used in the numerical solution in order to find grid independent results. It was found that a mesh with 200000 computational cells is sufficient for obtaining grid independent results (Fig. 5). The number of grids on each eclipse was 50, 100, and 200 in the three mesh sizes respectively.

The governing equations were integrated over each cell of the mesh and the resulting integrals were approximated using a multidimensional linear reconstruction approach (Ruge and Stuben, 1987). A computer code was developed to solve the discretized equations using algebraic multigrid method (Ruge and Stuben, 1987) and SIMPLE algorithm (Patankar, 1980). The central difference scheme and QUICK scheme were used for discretization of diffusive and convective terms, respectively (Leonard, 1995).

5. Results and discussion

Numerical analysis includes three parts in the range of air flow maximum Reynolds numbers 50-300. In the first part, the efficiency of different cases without metal foam inserts is compared with each other. After that, the best case is introduced and then streamline and temperature contours are presented for it. In the second part, all calculations are done for the cases with

metal foam inserts as well. In the last part, some of the results obtained from the two previous parts are compared.

In this work, five different geometries (cases) are used in the numerical analysis. Case 1 is our reference case. Cases 2-5 are similar cases in which the longitudinal and transverse pitches were changed according to limitations of our manufacturing devices in the heat exchanger factory. The geometric parameters for these cases are given in Table 3.

Table 2. Geometric parameters for five cases used in the numerical analysis

Case no.	S_T [cm]	S_L [cm]	Description
1	3.6	3.61	reference case
2	3.6	3.56	S_L is 1.3% less than that for the ref. case
3	3.6	3.71	S_L is 2.7% greater than that for the ref. case
4	3.2	3.61	S_T is 11% less than that for the ref. case
5	4.0	3.61	S_T is 11% greater than that for the ref. case

The total heat transfer rate from the tube bundle Q and the total pressure drop from row 1 to row 10, ΔP, are calculated using numerical results. For the cases with porous media inserts, three porous media with porosities $\varepsilon = 0.6, 0.8, 0.9$ are used in the numerical analysis. In the following figures, Re_{max} is the maximum Reynolds number between the tubes ($\mathrm{Re}_{max} = \rho V_{max} a / \mu$). The overall heat transfer efficiency of the tube bundle is defined as

$$efficiency = \frac{Q}{\Delta p} \left[\frac{\mathrm{W}}{\mathrm{Pa}} \right] \tag{5.1}$$

which seems to be a reasonable parameter to make comparisons between the various cases. Figure 6 shows a comparison between various cases without metal foam inserts.
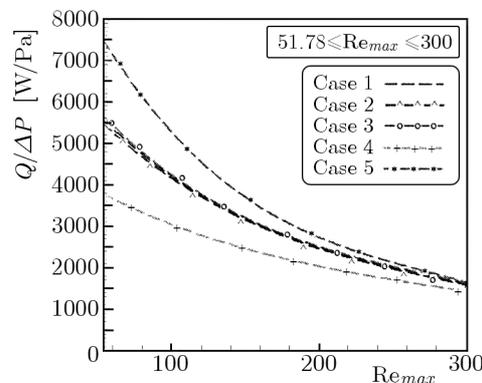
Fig. 6. The efficiency of five cases without metal foam inserts, $\mathrm{Pr} = 0.7$

It can be seen that case 5 has better efficiency than the other cases. On the other hand, this figure shows that the increasing of the transverse pitch S_T (as in case 5 with respect to case 1) is more effective than the other possible changes in the tube bundle arrangement for heat transfer efficiency enhancement. Figure 7 shows streamlines for case 5 at three maximum Reynolds numbers 51.78, 200, and 300.

It can be seen that the size of recirculation zones behind tubes grows by increasing the maximum Reynolds number. The temperature contours at the three Reynolds numbers are shown in Fig. 8.

It is clearly seen that temperature distribution changes by increasing the maximum Reynolds number. As the Reynolds number increases, the thermal boundary layer thickness on the tubes decreases and the convective heat transfer rate from tube rows increases. At low Reynolds
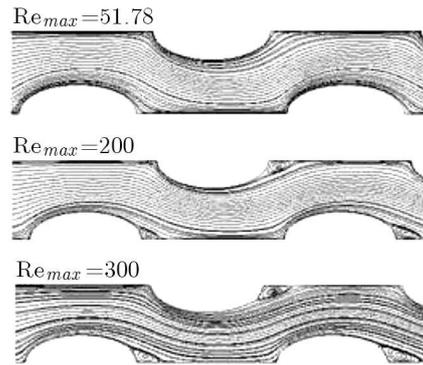
Fig. 7. Streamlines around tubes without metal foam insert for case 5
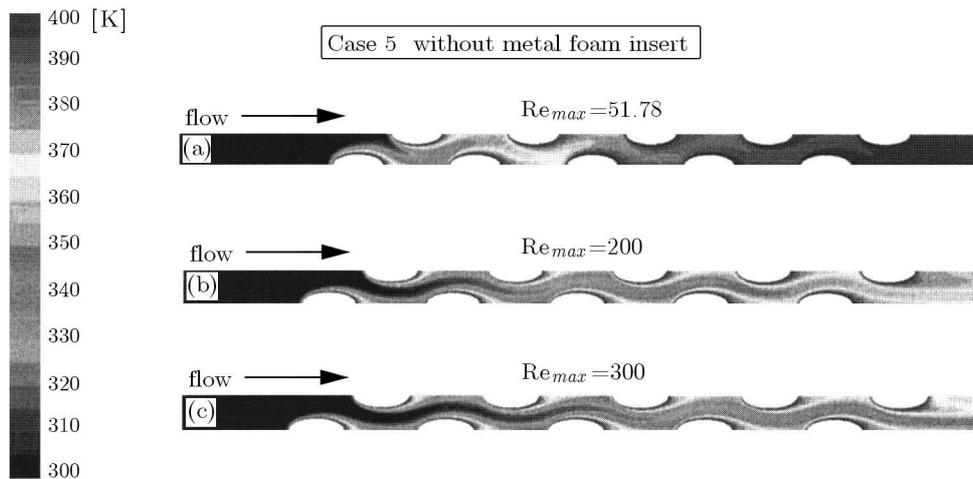
Fig. 8. Temperature contours around tubes at three different maximum Reynolds numbers without metal foam insert, $\mathrm{Pr} = 0.7$

numbers, the fluid core (the blue color region) warms up faster due to higher heat conduction or diffusion with respect to convection.

In the following part, the efficiency of the previous five cases with metal foam inserts is compared and the best case is introduced. Metal foams used here are aluminum foams with $k_{AL} = 237 \, \mathrm{W/(m\,K)}$, $C_s = 871 \, \mathrm{J/(kg\,K)}$, $\rho = 2719 \, \mathrm{kg/m^3}$ and their permeability K constant and equal to $10^{-8} \, \mathrm{m^2}$ and with the porosities $\varepsilon = 0.6$, 0.8, and 0.9. Also, the local thermal equilibrium condition is justified using the criterion given by Kim and Jang (2002). Figure 9 shows a comparison between various cases with an aluminum foam insert with permeability $10^{-8} \, \mathrm{m^2}$ and porosity 0.6.

It can be seen that similar to the previous part (without metal foam inserts), the best efficiency resulted when the tube transverse pitch was maximum. On the other hand, case 5 is the best case again. Figure 10 shows the effect of porosity on cases 3 and 5.

It is observed on both figures that the efficiency increases by decreasing porosity from 0.9 to 0.6 and Reynolds number from 300 to 50. It should be noted that these results are obtained at constant Permeability $10^{-8} \, \mathrm{m^2}$. Finally, the results for the best case (case 5) with and without aluminum foam inserts are compared with each other in Fig. 11. Here, the influence of pressure drop is neglected.

As it is shown in Fig. 11, the heat transfer increases by inserting metal foam among the tubes in the tube bundle. This is due to the high conductivity and surface area of aluminum foams. Figure 12 shows streamlines around the tubes with and without the aluminum foam inserts.
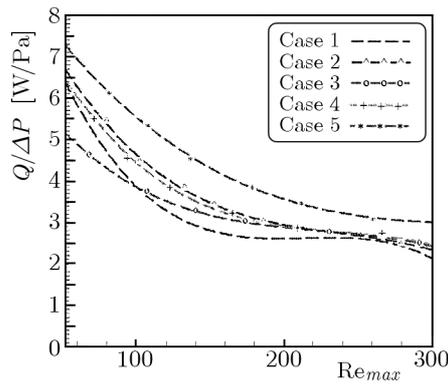
Fig. 9. The efficiency of five cases with an aluminum foam insert with $K = 10^{-8}\,\mathrm{m}^2$ and $\varepsilon = 0.6$, Pr = 0.7
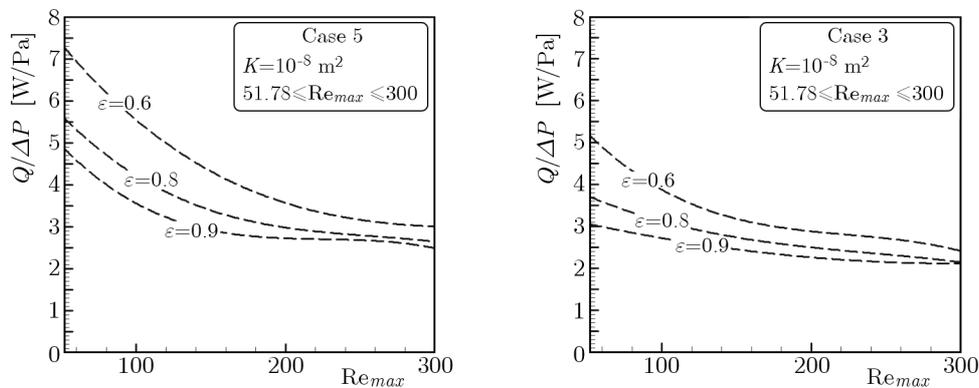
Fig. 10. The effect of porosity on the efficiency at constant permeability $K = 10^{-8}\,\mathrm{m}^2$, Pr = 0.7
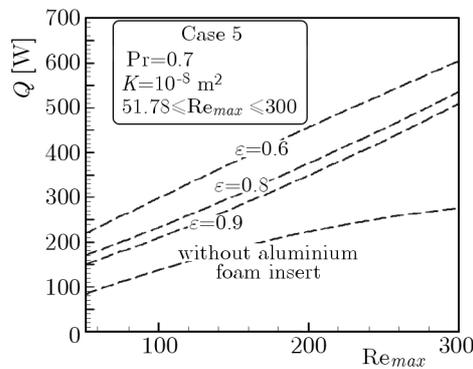
Fig. 11. A comparison between heat transfer rates with and without metal foam inserts for case 5
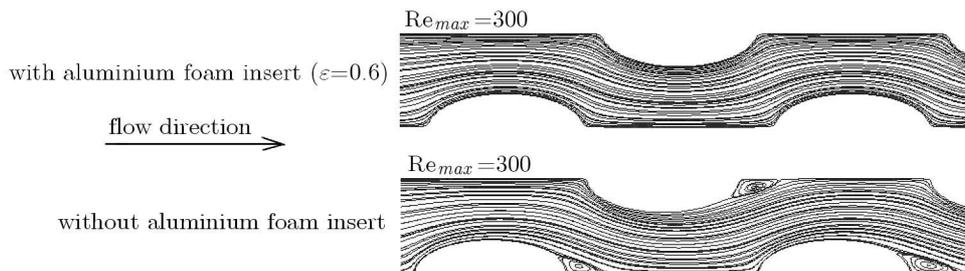
Fig. 12. Streamlines around tubes with or without aluminum foam inserts at $\mathrm{Re}_{max} = 300$

In the presence of aluminum foam inserts, the recirculation zones behind the tubes are much smaller than in the cases without the aluminum foam inserts. This is due to the effect of porous medium structure on the flow velocity gradients which prevents the creation of vortices behind the tubes. Therefore, it causes an increase in the heat transfer rate from the tubes.
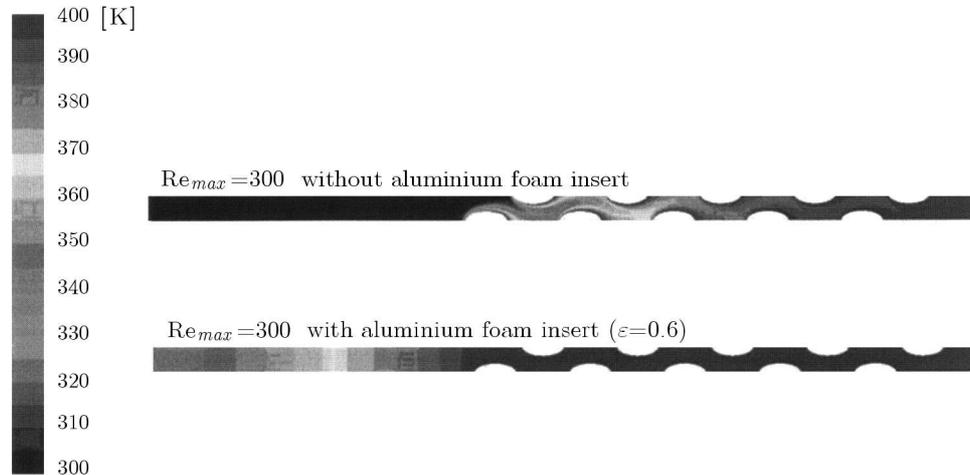
Fig. 13. A comparison of temperature contours with and without aluminum foam inserts

Figure 13 indicates that by inserting aluminum foam among the tubes, due to the increase of contact surface and thermal conductivity, the temperature distribution along the tube bundle changes quickly and heat transfer increases significantly. Similar results have been seen for the other cases.

Grid independency of the results has been checked in each case by running the computer code for three different mesh sizes, each one 50% finer than the other. Figure 14 shows the differences between these numerical results. The term "adapt1" refers to the first fine grid (with 200000 computational cells) used and the term "adapt2" refers to the second finer grid (with 800000 computational cells). The maximum difference between the numerical results was less than 1% in this case. Similar results have been obtained for the other cases as well.
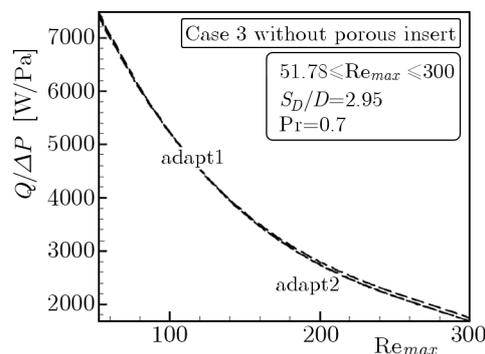
Fig. 14. Grid independency of numerical results at various Reynolds numbers

Our numerical results obtained by the computer code have also been validated against the results presented by Horvat *et al.* (2006) at Reynolds numbers less than 1000 for elliptical tube bundles. Here, the Stanton number is shown in Fig. 15. A good agreement can be noticed between the numerical results. The differences between the worst data were about 4%.
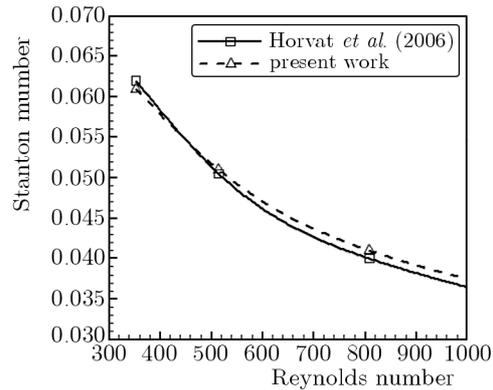
Fig. 15. A comparison between the numerical results for the Stanton number with the data given by Horvat *et al.* (2006) for tubes wit the pitch-to-diameter ratio 1.25 and hydraulic diameter of 0.9142 cm

6. Conclusion

In this paper, the effects of changeable transverse and longitudinal pitches and porous media inserts on heat transfer from an industrial elliptic tube bundle have been studied numerically. Aluminum foams have been used as porous media inserts between the tubes with three different porosities. It has been shown that using aluminum foam enhances heat transfer significantly (more than 50% in some cases). However, the pressure drop increases as the Reynolds number increases. Also, the differences in various cases have been discussed. The main conclusions of this research can be summarized as:

- With and without aluminum foam inserts, the enhanced heat transfer efficiency results when the tube transverse pitch is increased. This effect is stronger when compared to the varying longitudinal pitch.

- The total heat transfer rate and pressure drop both increase with decreasing porosity of metal foam inserts. Therefore, careful attention is needed in selecting appropriate metal foam inserts to obtain the best efficiency.

- Enhancement in the efficiency increases by decreasing the Reynolds number from 300 to 50. This means that metal foam inserts are more effective at lower Reynolds numbers.

- Heat transfer rate from the tubes in the bundle with metal foam inserts with porosity ranges between 0.6 to 0.9 is higher than that of the tubes in a bundle without metal foam inserts for all investigated cases.

- In the presence of aluminum foam inserts, the recirculation zones behind tubes is smaller than in the cases without aluminum foam inserts. Therefore, it causes an increase in the heat transfer rate from the tubes.

References

1. BASTAWROS A.F., 1998, Effectiveness of open-cell metallic foams for high power electronic cooling, *ASME Conference Proceedings HTD-361-3/PID-3*, 211-217

2. BERBISH N.S., 2011, Heat transfer and flow behavior around four staggered elliptic cylinders in cross flow, *Heat and Mass Transfer*, **47**, 3, 287-300

3. BHATTACHARYA A., MAHAJAN R. L., 2002, Finned metal foam heat sinks for electronic cooling in forced convection, *Journal of Electronic Packaging*, **124**, 3, 155-163

4. Bordalo S.N., Saboya F.E.M., 1999, Pressure drop coefficients for elliptic and circular sections in one, two and three-row arrangements of plate fin and tube heat exchangers, *Journal of Brazilian Society of Mechanical Sciences*, **21**, 4, 600-610

5. Chen H.T., Lai J.R., 2012, Study of heat transfer characteristics on the fin of two-row plate finned-tube heat exchangers, *International Journal of Heat and Mass Transfer*, **55**, 15/16, 4088-4095

6. Horvat A., Leskovar M., Mavko B., 2006, Comparison of heat transfer conditions in tube bundle cross-flow for different tube shapes, *International Journal of Heat and Mass Transfer*, **49**, 5, 1027-1038

7. Horvat A., Mavko B., 2006, Heat transfer conditions in flow across a bundle of cylindrical and ellipsoidal tubes, *Numerical Heat Transfer, Part A*, **49**, 7, 699-715

8. Ibrahim T. A., Gomaa A., 2009, Thermal performance criteria of elliptic tube bundle in cross flow, *International Journal of Thermal Sciences*, **48**, 11, 2148-2158

9. Jang J.Y., Yang J.Y., 1998, Experimental and 3-d numerical analysis of the thermal-hydraulic characteristics of elliptic finned-tube heat exchangers, *Heat Transfer Engineering*, **19**, 4, 55-67

10. Kim S.J., Jang S.P., 2002, Effects of the Darcy number, Prandtl number, and the Reynolds number on local thermal non-equilibrium, *International Journal of Heat and Mass Transfer*, **45**, 19, 3885-3896

11. Kim J.Y., Song T.H., 2002, Microscopic phenomena and macroscopic evaluation of heat transfer from plate fins/circular tube assembly using naphthalene sublimation technique, *International Journal of Heat and Mass Transfer*, **45**, 16, 3397-3404

12. Layeghi M., 2008, Numerical analysis of wooden porous media effects on heat transfer from a staggered tube bundle, *ASME Journal of Heat Transfer*, **130**, 1, 014501-1-6

13. Leonard B.P., 1995, Order of accuracy of quick and related convection-diffusion schemes, *Applied Mathematical Modelling*, **19**, 11, 640-653

14. Li Z., Davidson J.H., Mantell S.C., 2006, Numerical simulation of flow field and heat transfer of streamlined cylinders in cross flow, *ASME Journal of Heat Transfer*, **128**, 6, 564-570

15. Mahdi H., Lopez P., Fuentes A.A., Jones R., 2006, Thermal performance of aluminum-foam CPU heat exchangers, *International Journal of Energy Research*, **30**, 11, 851-860

16. Marchi C.H., 2007, Numerical solution of staggered circular tubes in two-dimensional laminar forced convection, Federal University of Parana – UFPR Department of Mechanical Engineering, 42-48

17. Matos R.S., Laursen T.A., Vargas J.V.C., Bejan A., 2004, Three-dimensional optimization of staggered finned circular and elliptic tubes in forced convection, *International Journal of Thermal Sciences*, **43**, 5, 477-487

18. Matos R.S., Vargas J.V.C., Laursen T.A., Bejan A., 2004, Optimally staggered finned circular and elliptic tubes in forced convection, *International Journal of Heat and Mass Transfer*, **47**, 6, 1347-1359

19. Patankar S.V., 1980, *Numerical Heat Transfer and Fluid Flow*, Hemisphere, New York

20. Pavel B.I., Mohamad A.A., 2004, Experimental investigation of the potential of metallic porous inserts in enhancing forced convective heat transfer, *ASME Journal of Heat Transfer*, **126**, 4, 540-545

21. Rocha L.A.O., Saboya F.E.M., Vargas J.V.C., 1997, A comparative study of elliptical and circular sections in one and two-row tubes and plate fin heat exchangers, *International Journal of Heat Fluid Flow*, **18**, 2, 247-252

22. Rosman E.C., Carajilescov P., Saboya F.E.M., 1984, Performance of tube of one and two-row tube and plate fin heat exchangers, *ASME Journal of Heat Transfer*, **106**, 3, 627-632

23. Ruge J., Stuben K., 1987, *Algebraic Multigrid in Multigrid Methods*, S. Mc-Cormick, ed., Vol. 3 of Frontiers in Applied Mathematics, SIAM, Philadelphia, ch. 4, 73-130

24. Shih W.H., Chiu W.C., Hsieh W.H., 2006, Height effect on heat transfer characteristics of aluminum-foam heat sinks, *ASME Journal of Heat Transfer*, **128**, 6, 530-537

25. Simo Tala J.V., Bougeard D., Russeil S., Harion J.-L., 2012, Tube pattern effect on thermal hydraulic characteristics in a two-rows finned-tube heat exchanger, *International Journal of Thermal Science*, **60**, 6, 225-235

26. Tadrist L., Miscevic M., Rahli O., Topin F., 2004, About the use of fibrous materials in compact heat exchangers, *Experimental Thermal and Fluid Science*, **28**, 2/3, 193-199

27. Talaat A.I., Abdalla G., 2009, Thermal performance criteria of elliptic tube bundle in cross flow, *International Journal of Thermal Science*, **48**, 2148-2158

28. Tao Y.B., He Y.L., Wu Z.G., Tao W.Q., 2007, Three-dimensional numerical study and field synergy principle analysis of wavy fin heat exchangers with elliptic tubes, *International Journal of Heat Fluid Flow*, **28**, 6, 1531-1544

29. Thirumalai Kannan K., Senthil Kumar B., 2011, Heat transfer and fluid flow analysis in plate-fin and tube heat exchangers with different shaped vortex generators, *International Journal of Soft Computing and Engineering*, **2**, 1, 2231-2307

30. T'Joen C., De Jaeger P., Huisseune H., Van Herzeele S., Vorst N., De Paepe M., 2010, Thermo-hydraulic study of a single row heat exchanger consisting of metal foam covered round tubes, *International Journal of Heat and Mass Transfer*, **53**, 15/16, 3262-3274

31. Torikoshi K., Xi G., Nakazawa Y., Asano H., 1994, Flow and heat transfer performance of a plate fin and tube heat exchanger (1st report: effect of fin pitch), *10th International Heat Transfer Conference*, paper 9-HE-16, 411-416

32. Webb R.L., 1980, Air-side heat transfer in finned tube heat exchangers, *Heat Transfer Engineering*, **1**, 3, 33-49

33. Zukauskas A., 1972, Heat transfer from tubes in cross flow, *Advances in Heat Transver*, **8**, 93-160